High-throughput Screening of the CoRE-MOF-2019 Database for CO_2 Capture from Wet Flue Gas: A Multi-Scale Modeling Strategy

Srinivasu Kancharlapalli [a, b, c] *and Randall Q. Snurr* [a] *

[a]Department of Chemical and Biological Engineering, Northwestern University, Evanston, Illinois 60208, United States.

[b]Theoretical Chemistry Section, Chemistry Division, Bhabha Atomic Research Centre, Trombay, Mumbai 400085, India.

[c]Homi Bhabha National Institute, Anushaktinagar, Mumbai 400094, India

KEYWORDS. CO_2 adsorption, Density Functional Theory, Metal-Organic Framework, MOF, Monte Carlo simulation.

ABSTRACT. Stabilizing the escalating CO_2 levels in the atmosphere is a grand challenge in view of increasing global demand for energy, the majority of which currently comes from burning of fossil fuels. Capturing CO_2 from point source emissions using solid adsorbents may play a part in meeting this challenge., and metal-organic frameworks (MOFs) are considered to be a promising class of materials for this purpose. It is important to consider the co-adsorption of water when designing materials for CO_2 capture from post-combustion flue gases. Computational high-throughput screening (HTS) is a powerful tool to identify top performing candidates for a particular application from a large materials database. Using a multi-scale modeling strategy that includes a machine learning model, density functional theory (DFT) calculations, force field optimization, and grand canonical Monte Carlo (GCMC) simulations, we carried out a systematic computational HTS of the all-solvent-removed version of the Computation-Ready Experimental Metal-Organic Framework (CoRE-MOF-2019) database for selective adsorption of CO_2 from a wet flue gas mixture. After initial screening based on the pore diameters, a total of 3703 unique MOFs from the database were considered for screening based on the force field interaction energies of CO_2, N_2, and H_2O molecules with the MOFs. MOFs showing stronger interaction with CO_2 compared to that with H_2O and N_2 were considered for next level of screening based on the interaction energies calculated from DFT. CO_2 selective MOFs from DFT screening were further screened using two-component (CO_2 and N_2) and finally three-component (CO_2, N_2 and H_2O) GCMC simulations to predict the CO_2 capacity and CO_2/N_2 selectivity. Our screening study identified MOFs that show selective CO_2 adsorption under wet flue gas conditions with significant CO_2 uptake capacity and CO_2/N_2 selectivity in the presence of water vapor. We also analyzed the nature of pore confinements responsible for the observed CO_2 selectivity.

INTRODUCTION

Increasing carbon dioxide (CO_2) levels in the atmosphere and resulting extreme weather conditions are a major problem around the globe.[1,2] CO_2 is the major greenhouse gas, and the primary source of anthropogenic CO_2 is the burning of fossil fuels.[2] Although the renewable energy sector is growing rapidly, its contribution to the overall energy supply today is not large in most countries, and some sectors of the economy are difficult to decarbonize.[1,3,4] CO_2 capture is considered to be an important technique which could be installed at stationary emission points to restrict the further increase of CO_2 levels in the atmosphere, but conventional capture through aqueous amine scrubbing is an energy intensive process.[5–7] CO_2 capture using solid adsorbents is considered a promising alternative to amine scrubbing, and robust solid sorbents with desired working capacity and selectivity are urgently needed.[8–11] Many publications have focused on the primary CO_2/N_2 separation, but the co-existence of water vapor in emission streams can lead to loss of CO_2 working capacity due to blocking of the adsorption sites by water.[12–14]

Metal-organic frameworks (MOFs), a class of crystalline porous materials composed of inorganic (metal or metal oxide) nodes and organic linkers, are reported to have potential applications in separation and storage of various important gases,[15–18] and there are several databases that report large numbers of MOF structures, including the Computation-Ready Experimental (CoRE) MOFs,[19] Cambridge Structural Database (CSD) MOFs,[20] Quantum MOFs (QMOFs),[21] hypothetical MOFs (hMOFs),[22] etc. In addition to these reported structures, the chemical space of MOFs is virtually unlimited due to the large number of possible combinations of linkers, nodes, and crystal topologies.[23,24] Computational high-throughput screening (HTS) is therefore a helpful technique to screen these large databases to find MOFs for specific application like CO_2 capture.[25–27] Though a good number of HTS studies on CO_2 capture using MOFs are reported, many of them focused on CO_2/N_2 mixtures[28–31] and did not take into account the presence

of water vapor. There are two major difficulties in simulating water adsorption in MOFs. First, there are uncertainties in the force field models and their ability to capture the unusual properties of water resulting from the characteristic hydrogen bonding networks. Second, Monte Carlo simulations of water adsorption sometimes exhibit extremely slow convergence, especially for hydrophobic pores.[32,33]

Several recent HTS studies have considered water vapor along with CO_2 and N_2. Li et al.[34] screened 5109 CoRE MOFs for CO_2 capture from wet flue gas mixtures, wherein the selectivity for CO_2/H_2O was assessed from the ratio of the calculated Henry's law constants (K_H) for CO_2 and H_2O using framework charges calculating with the extended charge equilibration (EQeq) method, which is a rapid but approximate method for obtaining framework atom charges. Comparison of the CO_2/H_2O selectivity in the top 15 MOFs from K_H calculated using two different charge methods, EQeq and DFT based Repeating Electrostatic Potential Extracted ATomic (REPEAT), revealed that the CO_2/H_2O selectivity values using EQeq charges was overestimated and the K_H of H_2O is more sensitive to the charge method than those of CO_2 and N_2. Li and coworkers[35] further demonstrated the importance of accurate atomic charges on computational HTS predictions by screening the CoRE MOF database with DDEC6 atomic charges. Coelho et al.[36] studied the effect of relative humidity (RH) on gas uptake using an alternate approach where MOFs were preloaded with water molecules at different RH through NVT (constant number of atoms, volume, and temperature) simulations followed by adsorption of other gas molecules through GCMC simulations. They showed that the CO_2 uptake at 40% RH was negligible in the MOFs considered. Erucar et al.[37] explored the impact of water vapor on the CO_2 separation performance of 13 top MOFs from their previous computational HTS studies through two different techniques, simulating the (1) ternary mixtures ($CO_2/CH_4/H_2O$ and $CO_2/N_2/H_2O$) in the MOFs and (2) binary

mixtures (CO_2/CH_4 and CO_2/N_2) in MOFs with preloaded water at 80% RH. A significant decrease in both the CO_2 and N_2 uptakes for the MOFs preloaded with water is reported due to the high affinity for water in all the top MOFs selected for CO_2/N_2 separation. In another interesting study, Boyd et al.[38] reported the data driven discovery of MOFs for CO_2 capture from wet flue gas mixture. Here, they screened a library of 325,000 computationally generated MOFs that were categorized into three classes depending on the pore shapes and CO_2 adsorption sites. MOFs with parallel aromatic rings separated by around 7 Å were proposed to be effective for CO_2 capture in the presence of water vapor, and the authors also reported the synthesis of such MOFs with optimal CO_2 binding sites, which showed minimal influence of water on the CO_2 capture capacity.

In the present study, we followed a multi-scale modeling strategy as depicted in Figure 1 for high-throughput screening of the all-solvent removed (ASR) version of the CoRE-MOF-2019 database[19] to identify the top MOFs for CO_2 capture under wet flue gas conditions. In view of the long computational hours required for simulating the adsorption of water in this large number of MOFs, we used the interaction energies of CO_2, N_2 and H_2O molecules with the MOFs calculated from classical force field minimizations followed by more accurate DFT calculations as the first two steps of the HTS study. To treat the Coulombic interactions accurately in the force field simulations, we used the atomic charges generated using our machine learning model, namely, partial atomic charges in metal−organic frameworks (PACMOF),[39] which was trained and tested previously using DDEC6 atomic charges.[40–42] Since the single-molecule interaction energies neglect important sorbate/sorbate interactions, finally, we calculated the loading capacity and selectivity in selected MOFs from the previous step at flue gas conditions using GCMC simulations, and top candidates with high CO_2 selectivity and CO_2 loading capacity under humid conditions were identified. In addition to screening the MOF database, we also attempted to

understand how the nature of the pore confinement affects the CO_2 selectivity and capacity in the presence of water vapor.

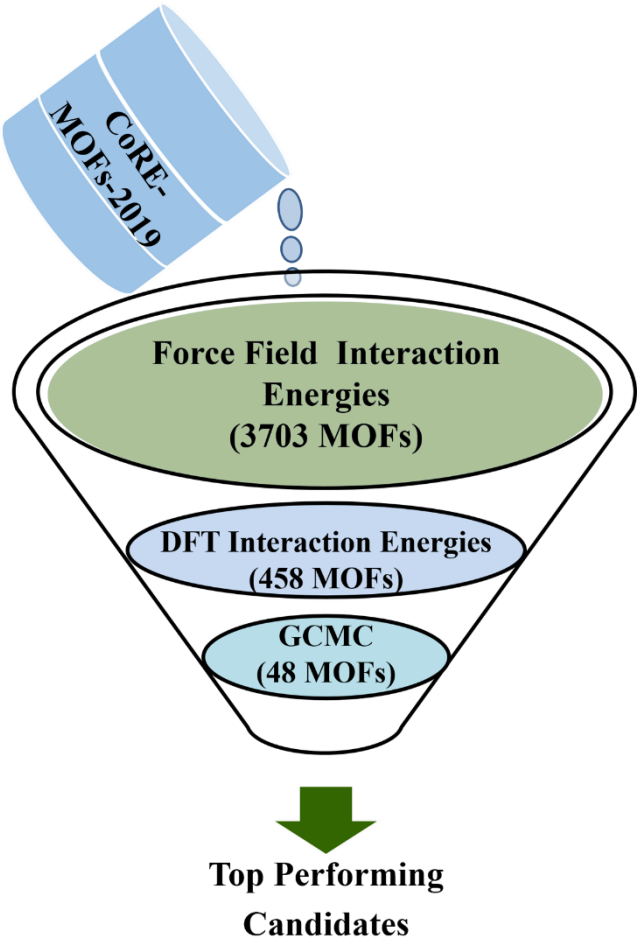

Figure 1: High-throughput screening procedure used on the CoRE-MOF-2019 database to identify top-performing materials for CO_2 capture under wet flue gas conditions.

Computational Methods

Selection of MOFs: For the HTS study, MOF structures were selected from the all-solvent-removed (ASR) version of the CoRE MOF-2019 database.[19] As the screening process involves computationally expensive DFT studies, we tried to limit the number of MOFs using different criteria as depicted in Figure S1. From the 14142 CoRE MOFs, the number was reduced to 7199 by considering only MOFs having largest cavity diameter (LCD) values up to 6 Å based on a previous study,[34] which reported that the MOFs with smaller pore sizes are more selective for CO_2 capture and also that large pore MOFs are not suitable for CO_2 capture at low partial pressures, such as those in flue gas. As a next condition, the maximum number of atoms per unit cell of MOF was limited to 500, due to the computationally expensive DFT calculations; this reduced the number of MOFs to 6967. Within these selected MOFs, some were found to have disorder or missing atoms, which we corrected manually followed by relaxation of the corrected structures using DFT at the PBE+D3 level of theory. The manually corrected structures are reported in the Supporting Information. MOF structures with missing charge balancing ions can lead to (incorrectly) charged unit cells, and the presence of extra-framework ions may also increase the hydrophilicity of the material. Hence, MOFs with charge-balancing ions were also exempted from the MOFs considered for HTS; this reduced the number of MOFs further to 4431. Since there were multiple MOFs with same structure and different CSD REFCODEs, we further screened for the presence of identical MOFs using the 'structure_matcher' module from the pymatgen software.[43] After exempting such identical MOFs, 3703 unique MOFs were considered for HTS.

Force Field Model: In the force field calculations (energy minimization and Monte Carlo simulations), the non-bonded interactions between atoms of the adsorbate molecules and the MOF atoms were modeled as a sum of Lennard−Jones (LJ) and Coulomb potentials

$$E_{ij} = 4\varepsilon_{ij}\left[\left(\frac{\sigma_{ij}}{r_{ij}}\right)^{12} - \left(\frac{\sigma_{ij}}{r_{ij}}\right)^{6}\right] + \frac{1}{4\pi\varepsilon_0}\frac{q_i q_j}{r_{ij}} \quad (1)$$

where r_{ij} is the distance between atoms i and j, σ_{ij} and ε_{ij} are the LJ parameters, and q_i is the partial atomic charge on atom i. The LJ parameters for the MOF atoms were taken from the universal force field (UFF),[44] and the cross interactions were calculated using the Lorentz−Berthelot mixing rules. A cut-off distance of 12.8 Å was considered for the LJ interactions without any tail correction, and sufficiently large super cells were considered to obey the minimum image convention. Partial atomic charges for the MOF atoms were assigned using the PACMOF[39] package, which was reported to give DDEC6 quality atomic charges. The LJ parameters and partial charges for guest molecules were treated using the TraPPE[45,46] (CO_2 and N_2) and TIP4P[47] (H_2O) force fields.

Force Field Optimization: To find the minimum energy adsorption configuration and calculate the interaction energy of the guest molecules (CO_2, H_2O and N_2) with the selected MOFs, 150 random initial configurations were generated for each molecule in each MOF. From each of these 150 configurations, the position of the guest molecule was optimized using the Baker minimization method as implemented in the RASPA package.[48]

DFT Calculations: Adsorption energies of guest molecules with the selected MOFs were calculated using spin-polarized periodic DFT calculations as implemented in the Vienna ab initio simulation package (VASP)[49–51] with a plane-wave kinetic energy cut-off of 520 eV. Projector augmented wave (PAW) potentials were used to treat the interactions between the core and valence electrons.[52] The exchange−correlation energy density functional was treated using the generalized gradient approximation (GGA) of Perdew, Burke, and Ernzerhof (PBE).[53] Grimme's DFT-D3 method with Becke-Johnson damping (PBE-D3) was used to treat the weak van der Waals interactions.[54] In view of the large number of calculations involved in the HTS and the large size of the MOF unit cells, only the Γ point was sampled in the Brillouin zone. Initial calculations

treated the framework atoms as fixed and optimized only the guest atom positions (so-called "selective dynamics"). For selected systems with stronger CO_2 interaction energy compared to the H_2O interaction energy at the DFT level, we also relaxed the MOF structures. A Hellmann−Feynman force cut-off of 0.01 eV $Å^{-1}$ was used for all the structural optimizations. Energies of the CO_2, H_2O, and N_2 molecules in the gas phase were calculated in a cubic cell of 15 Å length, and the interaction energy of guest molecule 'X' with the MOF was calculated as

$$\Delta E = E(X@MOF) - [E(MOF)+E(X)] \quad (2)$$

where E(X@MOF), E(MOF) and E(X) refer to energies of MOF with adsorbed guest molecule, empty MOF, and gas-phase molecule respectively.

GCMC Simulations: Although the DFT interaction energies should be more accurate than those calculated from the force field, these calculations considered only a single molecule interacting with the framework. To simulate the effect of loading of guest molecules beyond a single molecule, we studied the adsorption of binary (CO_2/N_2) and ternary ($CO_2/N_2/H_2O$) gas mixtures at the flue gas conditions using the grand canonical Monte Carlo (GCMC) simulation technique as implemented in the RASPA code.[48] For all MOFs selected from the previous screening step, we simulated the adsorption isotherm for a 15:85 mixture of CO_2 and N_2 at 313 K up to 1 bar total pressure. In a set of selected MOFs with high CO_2/N_2 selectivity and high CO_2 loading capacity from the binary mixture simulations, we simulated adsorption of a ternary mixture of $CO_2/N_2/H_2O$ at a relative humidity of 80% to test the effect of moisture on the CO_2/N_2 selectivity and CO_2 capacity. To calculate the relative humidity, the saturation pressure of water at 313 K was considered to be 7375 Pascals as per the reported results for TIP4P water by Vorholz et al.[55] For the binary mixtures, 50,000 Monte Carlo cycles were used for each equilibration and production considering insertion, deletion, translation, rotation, and identity change moves. A cycle is defined

as *N* move attempts, with *N* being the number of molecules in the system with a minimum of 20 moves per cycle. Since water adsorption is known to converge extremely slowly, we considered 1 x 10^6 cycles for both equilibration and production for the ternary mixtures. The selectivity for CO_2 over N_2 from GCMC simulations of binary and ternary gas mixtures was calculated as

$$Selectivity = \frac{\left({}^{n_{CO_2}}/_{p_{CO_2}}\right)}{\left({}^{n_{N_2}}/_{p_{N_2}}\right)} \qquad (3)$$

where *n* and *p* represent the uptake in mol/kg and the partial pressure, respectively. All HTS jobs were managed using the workflow managing code Fireworks.[56] Figures of the MOF structures were generated using the graphical software VESTA.[57]

Results and Discussion

For each MOF-guest molecule pair of 3703 MOFs and three guest molecules (CO_2, N_2 and H_2O), 150 random single molecule adsorption configurations were generated and optimized using the Baker optimization method, and the corresponding MOF-guest molecule interaction energies were calculated. Plots of the calculated N_2 versus CO_2 and H_2O versus CO_2 interaction energies using the force field methods are reported in Figure 2. It can be observed that most of the MOFs have a stronger interaction with CO_2 than with N_2 and a stronger interaction with water than with CO_2, as expected from the chemical nature of the guest molecules. Out of the 3703 MOFs considered, 458 MOFs are found to have stronger affinity toward CO_2 than toward both N_2 and H_2O.

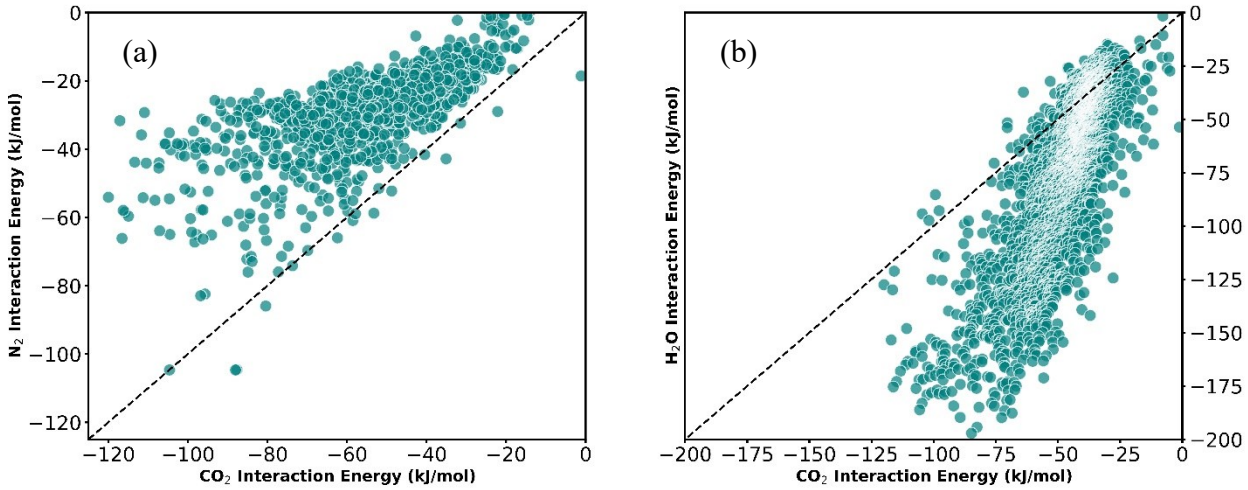

Figure 2: Interaction energies of MOFs with (a) CO_2 and N_2 and (b) CO_2 and H_2O molecules from force field energy minimizations.

After analysing the structures of the 458 MOFs selected based on the force field interaction energies, we found that some of them have either missing atoms or disordered atoms. These structures were consequently dropped from the computationally more expensive DFT screening, and only 387 MOFs were selected for DFT studies. For each of these 387 MOFs, the five lowest

energy adsorption configurations (from the force field interaction energies) for each molecule (CO_2, N_2 and H_2O) were considered as initial configurations for periodic DFT calculations using selective dynamics where the guest molecule alone is allowed to relax with fixed framework atoms. The energy of the lowest energy configuration from the five minimizations was used for calculating the interaction energy of the guest molecule with the MOF using equation 2. From the parity plots of the CO_2 and H_2O interaction energies calculated from force field and DFT methods in Figure 3, it can be observed that the CO_2 interaction energies (Figure 3a) are near the parity line for the majority of the MOFs. However, for H_2O interaction energies (Figure 3b), most of the MOFs are far from the parity line, and the DFT interaction energies are generally larger in magnitude than those from force field calculations, indicating that the water interaction energies from force field optimization were underestimated in many cases. Out of the 387 MOFs considered for DFT screening, 63 MOFs were found to have stronger interaction with CO_2 than with H_2O; parity plots of the interaction energies from force field and DFT studies on these 63 MOFs are reported in Figure S2.

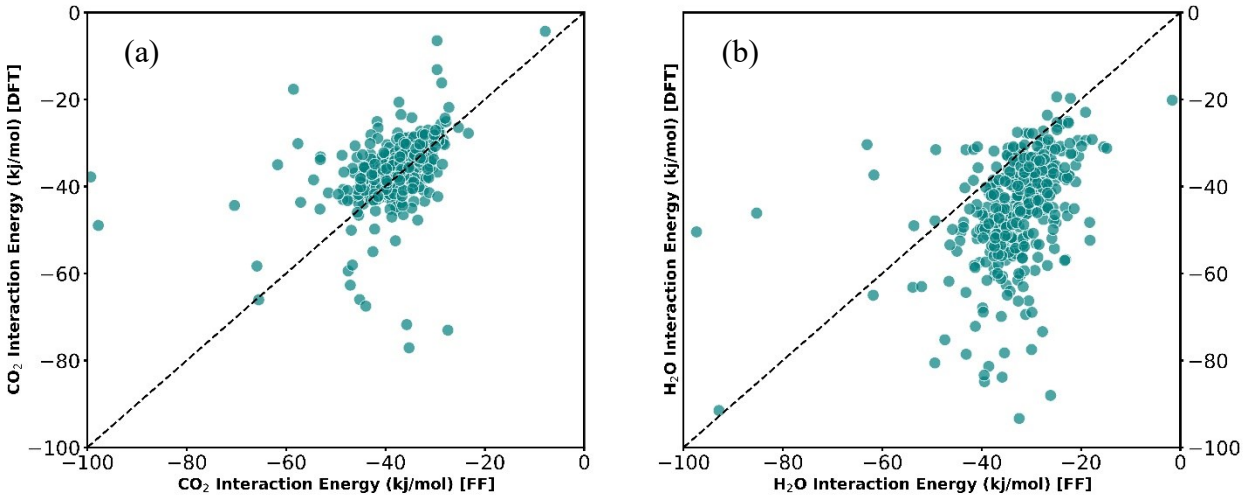

Figure 3. Interaction energies of MOFs with (a) CO_2 and (b) H_2O molecules with 387 selected MOFs calculated from force field (FF) and DFT methods.

For the 63 MOFs showing stronger CO_2 interactions than H_2O interactions, the lowest minimum energy adsorption configuration for each molecule (from the 5 configurations considered) was fully relaxed including relaxation of the framework atoms. Though the framework relaxation has minimal effect in many cases, in a few MOFs like OCEGUB (SIFSIX-3-Ni), we observed interesting effects. In most of the computational studies reported on SIFSIX-3-M MOFs,[58,59] the framework structures were considered as shown in Figure 4(a), which is the same as what we considered for the selective dynamics calculations. However, upon relaxing the framework atoms of SIFSIX-3-Ni with adsorbed water, the pyrazine rings were found to rotate to facilitate hydrogen bonding with the water molecule as shown in Figure 4(b), and, in fact, even for the pure MOF structure (with no adsorbed water) the structure with tilted pyrazine rings is found to be the minimum energy structure by an energy difference of 123.5 kJ/mol compared to the structure in 4(a). A similar transition of pyrazine rotational configurations in SIFSIX-3-M induced by Xe adsorption was reported by Elsaidi et al.[60] The SIFSIX-3-Ni structure in Figure 4(a) with fixed framework atoms was found to have stronger interaction with CO_2 compared to H_2O and the order of interaction energy was found to reverse upon the framework relaxation because of the strong hydrogen bonding environment in the pore for water adsorption. After considering the framework relaxation effect, 48 MOFs were found to have the stronger affinity for CO_2 than for H_2O.

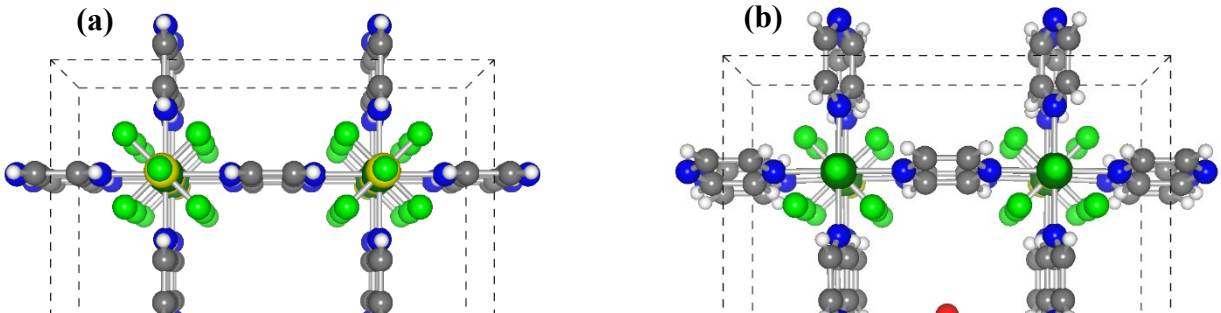

Figure 4. Optimized geometries of SIFSIX-3-Ni (a) without adsorbed water and (b) with adsorbed water.

Table 1: Top 20 MOFs with stronger CO_2 binding energy compared to H_2O binding energy calculated from periodic DFT studies after the framework atoms were relaxed.

MOF refcode	BE of CO_2 (kJ/mol)	BE of H_2O (kJ/mol)	ΔBE (kJ/mol)
CAYBAH01	-35.88	-24.34	11.54
RURPAW	-44.60	-33.14	11.46
CUIMDZ01	-45.72	-36.70	9.02
YUBFUX	-33.78	-25.63	8.15
ITAHEQ	-30.22	-22.19	8.03
RURPEA	-42.59	-34.72	7.87
FALQEQ	-34.15	-26.55	7.60
FALQOA	-33.97	-26.50	7.47
FALQIU	-33.97	-26.53	7.44
XENZEX	-37.69	-30.41	7.27
ZADWIN	-26.99	-20.68	6.30
NUYQUU	-41.37	-35.17	6.20
WOMCUY	-36.17	-30.24	5.94
RITDAB	-30.80	-26.23	4.57
SINZIA	-38.54	-34.37	4.17
PAPXUB	-35.13	-31.11	4.02
PIHJOH01	-34.82	-31.16	3.66
MUVGUG	-33.45	-30.00	3.45

EMUYAM01	-35.16	-31.82	3.34
AMUCOB	-31.06	-27.75	3.31

The top 20 MOFs showing high affinity towards CO_2 compared to H_2O from the DFT studies are tabulated in Table 1 along with their binding energies. The full list of all 48 MOFs is provided in Table S1. We also compared the computed minimum energy adsorption sites of CO_2 with reported experimental studies in a few MOFs. For example, in ZIF-7 (RIPNUB), which has two different cavities ('A type' and 'B type'), CO_2 was reported to preferentially occupy the 'B type' cavity, and our optimized minimum energy configuration reported in Figure S3(a) is consistent with the reported result.[61] Similarly, in the case of SIFSIX-3-Ni (OCEGUB), our DFT calculations predict that CO_2 adsorbs along the one-dimensional channel with the C_∞ axis of CO_2 along the C_4 axis of the lattice as reported in Fire S3(b) such that the positively charged carbon atom of CO_2 interacts with the framework halogen sites while the negatively charged oxygen atoms of CO_2 interact with the framework pyrazine hydrogen atoms, which is consistent with the experimentally reported results from in situ PXRD.[62]

We also examined the nature of the pore environment around the adsorption sites in the CO_2-selective MOFs to understand the observed strong affinity for CO_2 over H_2O and to provide insights for the design of improved porous materials for CO_2 capture under humid conditions. We mainly observed two chemical confinements that drive the observed affinity for CO_2 over H_2O, namely pores with (1) complementary charged sites to the atomic charges in the CO_2 molecule and (2) parallel cyclic aromatic (π) ligands separated by around 7 Å. In the former case, MOFs like YUBFUX[63] (Figure S4) have framework atomic charges that create an optimal site for strong Coulombic attraction with the CO_2 molecule while there were no such strong Columbic interactions for water adsorption. In an earlier study by Deria et al.,[64] it was reported that the

incorporation of complementary organic motifs in MOFs with precise charge alignment complementary to CO_2 atomic charges can enhance the CO_2 uptake. In the later type of confinement shown in MOFs like HIMSAY/BUSQEM[65,66] and RITDAB[67] (Figure S5), CO_2 binding is driven by the strong π-π interactions between the π electron systems of the aromatic ligands and the CO_2 molecule. To verify the optimum separation between the parallel aromatic rings, we calculated the CO_2 binding energy from DFT when placed between two pyrene rings at various fixed separation distances as shown in Figure S6. The results indicate that a separation distance of 6.8 Å is the optimum for CO_2 binding, and the corresponding binding energy is calculated to be -25.0 kJ/mol. Interestingly, this optimum separation is nearly double the interlayer separation in graphite, and hence it can be visualized as replacing one of the graphene layers in graphite with CO_2, which also has π electrons and can have similar π-π interactions as those present in graphite. Our findings are consistent with the reported results of Boyd et al.[38] where MOFs with parallel aromatic rings separated by around 6.7 Å were reported to show negligible effect of water on CO_2 uptake. Our explanation in terms of π-π interactions is further supported by a previously reported DFT study on CO_2 adsorption in single walled carbon nanotubes of different sizes, where a (9, 0) CNT with a diameter of 7.05 Å was shown to have the strongest CO_2 interaction energy compared to other CNTs with lower or higher diameters.[68]

To estimate the adsorbed phase loadings under flue gas conditions, we first used GCMC simulations to predict the adsorption isotherms of a binary mixture of CO_2 and N_2 in a 15:85 ratio at 313 K and 0.1 bar to 1 bar total pressure in the 48 selected MOFs from the previous screening step. From the binary mixture adsorption studies, only 10 MOFs are observed to show a reasonably high CO_2/N_2 selectivity and CO_2 uptake capacity as reported in Table S2. These materials were

then considered for the simulation of the ternary mixture. In the ternary adsorption studies, we fixed the partial pressure of water at 80% relative humidity (5900 Pa at 313 K) based on the saturation pressure reported for the TIP4P water model.[55,69] For the three-component adsorption, we simulated only at three pressures (sum of the partial pressures of CO_2 and N_2 with 15:85 composition), namely 0.1 bar, 0.5 bar, and 1.0 bar. In some cases, where the fluctuations in the loading were high even after 2 x 10^6 cycles, we extended the simulations for another 1 x 10^6 cycles. The simulated two- and three-component isotherms of the top 6 MOFs are reported in Figure 5. while the isotherms for the remaining MOFs are reported in Figure S7. From the ternary mixture simulation studies, the presence of water is found to have a negligible effect on the CO_2 uptake and CO_2/N_2 selectivity with the exception of GAYGAQ,[70] which has one-dimensional channels, where adsorbed water forms hydrogen bonded chains. Since the error bars in gas loading values calculated as the 95% confidence interval are smaller than the marker size, they were not reported in the isotherm plots.

We also studied both two and three component adsorption in two MOFs, SIFSIX-3-Ni (OCEGUB02) and NbOFFIVE-1-Ni (OWIKAI), in which water adsorption leads to rotation of pyrazine rings by considering both the structures with and without the ring rotation. The isotherms are reported in Figure S8, and it can be observed that the CO_2 uptake from both two and three component simulations in the structures with rotated pyrazine rings is lower compared to that in the structures with symmetrically oriented pyrazine rings (as in Figure 4(a)). The presence of water was found to reduce the CO_2 uptake in OWIKAI, while the effect was minimal in OCEGUB01.

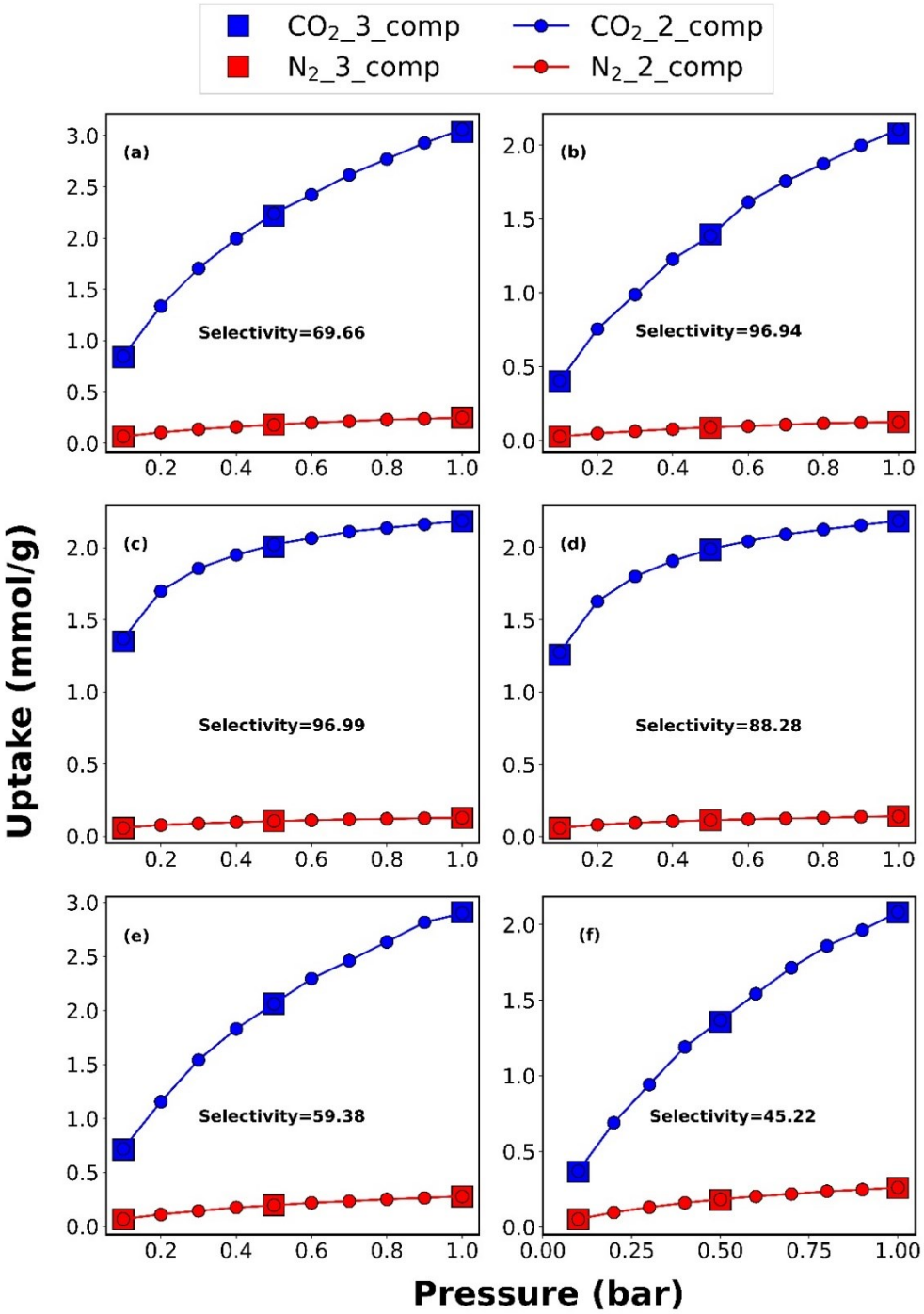

Figure 5.

Two- and three-component adsorption isotherms at 313 K for the top 6 MOFs identified from the screening process: (a) HIMSAY, (b) LUFQUZ, (c) RIPNUB, (d) VEJZEQ, (e) BUSQEM and (f) EREFEN01. The selectivity is calculated at 1 bar pressure with 80% relative humidity.

Conclusion

We carried out a systematic computational high-throughput screening study to identify the top performing MOFs from the CoRE-MOF-2019 database for CO_2 capture from a wet flue gas mixture. Multi-scale computational techniques, viz. a machine learning model to quickly obtain MOF partial atomic charges, force field optimization, DFT studies, and GCMC simulations were used for the HTS study. Screening using the force field interactions calculated between the MOF and guest molecules was able to reduce the number of MOFs to be studied using the computationally more expensive DFT studies. From the DFT studies, it was observed that framework relaxation can alter the selectivity in certain MOFs where ligand rotations are induced by guest molecule adsorption. Preferred adsorption sites for guest molecules were compared with experimental results where available and found to be consistent. For the top selected MOFs from the DFT screening, grand canonical Monte Carlo simulations were used to study the adsorption on both two- (CO_2 and N_2) and three-component mixtures (CO_2, N_2 and H_2O at 80% relative humidity). For the 10 MOFs where three-component adsorption simulations were performed, only one MOF showed reduced CO_2 uptake and CO_2/N_2 selectivity from the presence of water, validating the screening process. In addition to screening to find the top candidates, we also used the simulation results to understand the nature of pore confinement that is responsible for the observed CO_2/H_2O selectivity. Most of the selective MOFs have either strong π- π confinement from pores with parallel aromatic rings or confinement with framework atom charges that are complementary to the CO_2 atomic charges. These design rules may allow for the future synthesis of improved materials for CO_2 capture.

ASSOCIATED CONTENT

Supporting Information.

The following files are available free of charge.

DFT optimized structures of guest molecule adsorbed in the MOFs YUBFUX and BUSQEM, CO_2 under π-π confinement studies, and details of top 10 MOFs considered for three component adsorption studies (PDF)

cif of all the manually cleaned MOF structures (tar.gz)

List of manually cleaned MOF ref codes (xlsx)

CO_2, N_2 and H_2O interaction energies of all the MOFs from force field simulations (xlsx)

Two component adsorption isotherm data for 48 MOFs as csv files (tar.gz)

AUTHOR INFORMATION

Corresponding Author

*E-mail: snurr@northwestern.edu

Author Contributions

S. K. initiated the project and performed all the calculations. R. Q. S. initiated, supervised and guided the project. S. K. and R. Q. S. wrote the manuscript.

Funding Sources

R. Q. S. acknowledges funding from the U.S. National Science Foundation (Award No. 2119433).

ACKNOWLEDGMENT

S. K. thanks the United States-India Education Foundation (USIEF) and the Institute of International Education (IIE) for his Fulbright Nehru Postdoctoral Research Fellowship (Award#2396/FNPDR/2018). This research was supported in part through the computational resources and staff contributions provided for the Quest high performance computing facility at Northwestern University which is jointly supported by the Office of the Provost, the Office for Research, and Northwestern University Information Technology. S. K. thanks the Computer Division, BARC for providing the high-performance parallel computing facility

REFERENCES

(1) Lewis, N. S.; Nocera, D. G. Powering the Planet: Chemical Challenges in Solar Energy Utilization. *Proc. Natl. Acad. Sci.* **2006**, *103* (43), 15729–15735. https://doi.org/10.1073/pnas.0603395103.

(2) Mac Dowell, N.; Fennell, P. S.; Shah, N.; Maitland, G. C. The Role of CO2 Capture and Utilization in Mitigating Climate Change. *Nat. Clim. Change* **2017**, *7* (4), 243–249. https://doi.org/10.1038/nclimate3231.

(3) Fang, H.; Demir, H.; Kamakoti, P.; Sholl, D. S. Recent Developments in First-Principles Force Fields for Molecules in Nanoporous Materials. *J. Mater. Chem. A* **2014**, *2* (2), 274–291. https://doi.org/10.1039/C3TA13073H.

(4) Yue, M.; Lambert, H.; Pahon, E.; Roche, R.; Jemei, S.; Hissel, D. Hydrogen Energy Systems: A Critical Review of Technologies, Applications, Trends and Challenges. *Renew. Sustain. Energy Rev.* **2021**, *146*, 111180. https://doi.org/10.1016/j.rser.2021.111180.

(5) Joos, L.; Huck, J. M.; Speybroeck, V. V.; Smit, B. Cutting the Cost of Carbon Capture: A Case for Carbon Capture and Utilization. *Faraday Discuss.* **2016**, *192* (0), 391–414. https://doi.org/10.1039/C6FD00031B.

(6) Leung, D. Y. C.; Caramanna, G.; Maroto-Valer, M. M. An Overview of Current Status of Carbon Dioxide Capture and Storage Technologies. *Renew. Sustain. Energy Rev.* **2014**, *39*, 426–443. https://doi.org/10.1016/j.rser.2014.07.093.

(7) Rochelle, G. T. Amine Scrubbing for CO2 Capture. *Science* **2009**, *325* (5948), 1652–1654. https://doi.org/10.1126/science.1176731.

(8) Wang, Q.; Luo, J.; Zhong, Z.; Borgna, A. CO2 Capture by Solid Adsorbents and Their Applications: Current Status and New Trends. *Energy Environ. Sci.* **2011**, *4* (1), 42–55. https://doi.org/10.1039/C0EE00064G.

(9) Siegelman, R. L.; Kim, E. J.; Long, J. R. Porous Materials for Carbon Dioxide Separations. *Nat. Mater.* **2021**, *20* (8), 1060–1072. https://doi.org/10.1038/s41563-021-01054-8.

(10) Pera-Titus, M. Porous Inorganic Membranes for CO2 Capture: Present and Prospects. *Chem. Rev.* **2014**, *114* (2), 1413–1492. https://doi.org/10.1021/cr400237k.

(11) Farmahini, A. H.; Krishnamurthy, S.; Friedrich, D.; Brandani, S.; Sarkisov, L. Performance-Based Screening of Porous Materials for Carbon Capture. *Chem. Rev.* **2021**, *121* (17), 10666–10741. https://doi.org/10.1021/acs.chemrev.0c01266.

(12) Kolle, J. M.; Fayaz, M.; Sayari, A. Understanding the Effect of Water on CO2 Adsorption. *Chem. Rev.* **2021**, *121* (13), 7280–7345. https://doi.org/10.1021/acs.chemrev.0c00762.

(13) Kizzie, A. C.; Wong-Foy, A. G.; Matzger, A. J. Effect of Humidity on the Performance of Microporous Coordination Polymers as Adsorbents for CO2 Capture. *Langmuir* **2011**, *27* (10), 6368–6373. https://doi.org/10.1021/la200547k.

(14) Chanut, N.; Bourrelly, S.; Kuchta, B.; Serre, C.; Chang, J.-S.; Wright, P. A.; Llewellyn, P. L. Screening the Effect of Water Vapour on Gas Adsorption Performance: Application to CO2 Capture from Flue Gas in Metal–Organic Frameworks. *ChemSusChem* **2017**, *10* (7), 1543–1553. https://doi.org/10.1002/cssc.201601816.

(15) Bharadwaj, P. K.; Feng, P.; Kaskel, S.; Xu, Q. Metal–Organic Frameworks and Their Applications. *Chem. – Asian J.* **2019**, *14* (20), 3450–3451. https://doi.org/10.1002/asia.201901288.

(16) Zhou, H.-C.; Long, J. R.; Yaghi, O. M. Introduction to Metal–Organic Frameworks. *Chem. Rev.* **2012**, *112* (2), 673–674. https://doi.org/10.1021/cr300014x.

(17) Li, H.; Eddaoudi, M.; O'Keeffe, M.; Yaghi, O. M. Design and Synthesis of an Exceptionally Stable and Highly Porous Metal-Organic Framework. *Nature* **1999**, *402* (6759), 276–279. https://doi.org/10.1038/46248.

(18) Kancharlapalli, S.; Natarajan, S.; Ghanty, T. K. Confinement-Directed Adsorption of Noble Gases (Xe/Kr) in MFM-300(M)-Based Metal–Organic Framework Materials. *J. Phys. Chem. C* **2019**, *123* (45), 27531–27541. https://doi.org/10.1021/acs.jpcc.9b06961.

(19) Chung, Y. G.; Haldoupis, E.; Bucior, B. J.; Haranczyk, M.; Lee, S.; Zhang, H.; Vogiatzis, K. D.; Milisavljevic, M.; Ling, S.; Camp, J. S.; Slater, B.; Siepmann, J. I.; Sholl, D. S.; Snurr, R. Q. Advances, Updates, and Analytics for the Computation-Ready, Experimental Metal–Organic Framework Database: CoRE MOF 2019. *J. Chem. Eng. Data* **2019**, *64* (12), 5985–5998. https://doi.org/10.1021/acs.jced.9b00835.

(20) Moghadam, P. Z.; Li, A.; Wiggin, S. B.; Tao, A.; Maloney, A. G. P.; Wood, P. A.; Ward, S. C.; Fairen-Jimenez, D. Development of a Cambridge Structural Database Subset: A Collection of Metal–Organic Frameworks for Past, Present, and Future. *Chem. Mater.* **2017**, *29* (7), 2618–2625. https://doi.org/10.1021/acs.chemmater.7b00441.

(21) Rosen, A. S.; Iyer, S. M.; Ray, D.; Yao, Z.; Aspuru-Guzik, A.; Gagliardi, L.; Notestein, J. M.; Snurr, R. Q. Machine Learning the Quantum-Chemical Properties of Metal–Organic Frameworks for Accelerated Materials Discovery. *Matter* **2021**, *4* (5), 1578–1597. https://doi.org/10.1016/j.matt.2021.02.015.

(22) Wilmer, C. E.; Leaf, M.; Lee, C. Y.; Farha, O. K.; Hauser, B. G.; Hupp, J. T.; Snurr, R. Q. Large-Scale Screening of Hypothetical Metal–Organic Frameworks. *Nat Chem* **2012**, *4* (2), 83–89. https://doi.org/10.1038/nchem.1192.

(23) Colón, Y. J.; Gómez-Gualdrón, D. A.; Snurr, R. Q. Topologically Guided, Automated Construction of Metal–Organic Frameworks and Their Evaluation for Energy-Related Applications. *Cryst. Growth Des.* **2017**, *17* (11), 5801–5810. https://doi.org/10.1021/acs.cgd.7b00848.

(24) Boyd, P. G.; Woo, T. K. A Generalized Method for Constructing Hypothetical Nanoporous Materials of Any Net Topology from Graph Theory. *CrystEngComm* **2016**, *18* (21), 3777–3792. https://doi.org/10.1039/C6CE00407E.

(25) Avci, G.; Velioglu, S.; Keskin, S. High-Throughput Screening of MOF Adsorbents and Membranes for H2 Purification and CO2 Capture. *ACS Appl. Mater. Interfaces* **2018**, *10* (39), 33693–33706. https://doi.org/10.1021/acsami.8b12746.

(26) Banerjee, D.; Simon, C. M.; Plonka, A. M.; Motkuri, R. K.; Liu, J.; Chen, X.; Smit, B.; Parise, J. B.; Haranczyk, M.; Thallapally, P. K. Metal–Organic Framework with Optimally Selective Xenon Adsorption and Separation. *Nat. Commun.* **2016**, *7* (1), ncomms11831. https://doi.org/10.1038/ncomms11831.

(27) Colón, Y. J.; Snurr, R. Q. High-Throughput Computational Screening of Metal–Organic Frameworks. *Chem. Soc. Rev.* **2014**, *43* (16), 5735–5749. https://doi.org/10.1039/C4CS00070F.

(28) Haldoupis, E.; Nair, S.; Sholl, D. S. Finding MOFs for Highly Selective CO2/N2 Adsorption Using Materials Screening Based on Efficient Assignment of Atomic Point Charges. *J. Am. Chem. Soc.* **2012**, *134* (9), 4313–4323. https://doi.org/10.1021/ja2108239.

(29) Li, S.; Chung, Y. G.; Simon, C. M.; Snurr, R. Q. High-Throughput Computational Screening of Multivariate Metal–Organic Frameworks (MTV-MOFs) for CO2 Capture. *J. Phys. Chem. Lett.* **2017**, *8* (24), 6135–6141. https://doi.org/10.1021/acs.jpclett.7b02700.

(30) Altintas, C.; Avci, G.; Daglar, H.; Nemati Vesali Azar, A.; Velioglu, S.; Erucar, I.; Keskin, S. Database for CO2 Separation Performances of MOFs Based on Computational Materials Screening. *ACS Appl. Mater. Interfaces* **2018**, *10* (20), 17257–17268. https://doi.org/10.1021/acsami.8b04600.

(31) Dickey, A. N.; Yazaydın, A. Ö.; Willis, R. R.; Snurr, R. Q. Screening CO2/N2 Selectivity in Metal-Organic Frameworks Using Monte Carlo Simulations and Ideal Adsorbed Solution Theory. *Can. J. Chem. Eng.* **2012**, *90* (4), 825–832. https://doi.org/10.1002/cjce.20700.

(32) Castillo, J. M.; Dubbeldam, D.; Vlugt, T. J. H.; Smit, B.; Calero, S. Evaluation of Various Water Models for Simulation of Adsorption in Hydrophobic Zeolites. *Mol. Simul.* **2009**, *35* (12–13), 1067–1076. https://doi.org/10.1080/08927020902865923.

(33) Sarkisov, L.; Centineo, A.; Brandani, S. Molecular Simulation and Experiments of Water Adsorption in a High Surface Area Activated Carbon: Hysteresis, Scanning Curves and Spatial Organization of Water Clusters. *Carbon* **2017**, *118*, 127–138. https://doi.org/10.1016/j.carbon.2017.03.044.

(34) Li, S.; Chung, Y. G.; Snurr, R. Q. High-Throughput Screening of Metal–Organic Frameworks for CO2 Capture in the Presence of Water. *Langmuir* **2016**, *32* (40), 10368–10376. https://doi.org/10.1021/acs.langmuir.6b02803.

(35) Li, W.; Rao, Z.; Chung, Y. G.; Li, S. The Role of Partial Atomic Charge Assignment Methods on the Computational Screening of Metal-Organic Frameworks for CO2 Capture under Humid Conditions. *ChemistrySelect* **2017**, *2* (29), 9458–9465. https://doi.org/10.1002/slct.201701934.

(36) Coelho, J. A.; Lima, A. E. O.; Rodrigues, A. E.; Azevedo, D. C. S.; Lucena, S. M. P. Computer Simulation of Adsorption and Sitting of CO2, N2, CH4 and Water on a New Al(OH)-Fumarate MOF. *Adsorption* **2017**, *2–3* (23), 423–431. https://doi.org/10.1007/s10450-017-9872-7.

(37) Erucar, I.; Keskin, S. Unlocking the Effect of H2O on CO2 Separation Performance of Promising MOFs Using Atomically Detailed Simulations. *Ind. Eng. Chem. Res.* **2020**, *59* (7), 3141–3152. https://doi.org/10.1021/acs.iecr.9b05487.

(38) Boyd, P. G.; Chidambaram, A.; García-Díez, E.; Ireland, C. P.; Daff, T. D.; Bounds, R.; Gładysiak, A.; Schouwink, P.; Moosavi, S. M.; Maroto-Valer, M. M.; Reimer, J. A.; Navarro, J. A. R.; Woo, T. K.; Garcia, S.; Stylianou, K. C.; Smit, B. Data-Driven Design of Metal–Organic Frameworks for Wet Flue Gas CO 2 Capture. *Nature* **2019**, *576* (7786), 253–256. https://doi.org/10.1038/s41586-019-1798-7.

(39) Kancharlapalli, S.; Gopalan, A.; Haranczyk, M.; Snurr, R. Q. Fast and Accurate Machine Learning Strategy for Calculating Partial Atomic Charges in Metal–Organic Frameworks. *J. Chem. Theory Comput.* **2021**, *17* (5), 3052–3064. https://doi.org/10.1021/acs.jctc.0c01229.

(40) Manz, T. A.; Limas, N. G. Introducing DDEC6 Atomic Population Analysis: Part 1. Charge Partitioning Theory and Methodology. *RSC Adv.* **2016**, *6* (53), 47771–47801. https://doi.org/10.1039/C6RA04656H.

(41) Limas, N. G.; Manz, T. A. Introducing DDEC6 Atomic Population Analysis: Part 2. Computed Results for a Wide Range of Periodic and Nonperiodic Materials. *RSC Adv.* **2016**, *6* (51), 45727–45747. https://doi.org/10.1039/C6RA05507A.

(42) Limas, N. G.; Manz, T. A. Introducing DDEC6 Atomic Population Analysis: Part 4. Efficient Parallel Computation of Net Atomic Charges, Atomic Spin Moments, Bond Orders, and More. *RSC Adv.* **2018**, *8* (5), 2678–2707. https://doi.org/10.1039/C7RA11829E.

(43) Ong, S. P.; Richards, W. D.; Jain, A.; Hautier, G.; Kocher, M.; Cholia, S.; Gunter, D.; Chevrier, V. L.; Persson, K. A.; Ceder, G. Python Materials Genomics (Pymatgen): A Robust, Open-Source Python Library for Materials Analysis. *Comput. Mater. Sci.* **2013**, *68*, 314–319. https://doi.org/10.1016/j.commatsci.2012.10.028.

(44) Rappe, A. K.; Casewit, C. J.; Colwell, K. S.; Goddard, W. A.; Skiff, W. M. UFF, a Full Periodic Table Force Field for Molecular Mechanics and Molecular Dynamics Simulations. *J. Am. Chem. Soc.* **1992**, *114* (25), 10024–10035. https://doi.org/10.1021/ja00051a040.

(45) Potoff, J. J.; Siepmann, J. I. Vapor–Liquid Equilibria of Mixtures Containing Alkanes, Carbon Dioxide, and Nitrogen. *AIChE J.* **2001**, *47* (7), 1676–1682. https://doi.org/10.1002/aic.690470719.

(46) Eggimann, B. L.; Sun, Y.; DeJaco, R. F.; Singh, R.; Ahsan, M.; Josephson, T. R.; Siepmann, J. I. Assessing the Quality of Molecular Simulations for Vapor–Liquid Equilibria: An Analysis of the TraPPE Database. *J. Chem. Eng. Data* **2020**, *65* (3), 1330–1344. https://doi.org/10.1021/acs.jced.9b00756.

(47) Jorgensen, W. L.; Chandrasekhar, J.; Madura, J. D.; Impey, R. W.; Klein, M. L. Comparison of Simple Potential Functions for Simulating Liquid Water. *J. Chem. Phys.* **1983**, *79* (2), 926–935. https://doi.org/10.1063/1.445869.

(48) Dubbeldam, D.; Calero, S.; Ellis, D. E.; Snurr, R. Q. RASPA: Molecular Simulation Software for Adsorption and Diffusion in Flexible Nanoporous Materials. *Mol. Simul.* **2016**, *42* (2), 81–101. https://doi.org/10.1080/08927022.2015.1010082.

(49) Kresse, G.; Furthmüller, J. Efficiency of Ab-Initio Total Energy Calculations for Metals and Semiconductors Using a Plane-Wave Basis Set. *Comput. Mater. Sci.* **1996**, *6* (1), 15–50. https://doi.org/10.1016/0927-0256(96)00008-0.

(50) Kresse, G.; Furthmüller, J. Efficient Iterative Schemes for Ab Initio Total-Energy Calculations Using a Plane-Wave Basis Set. *Phys. Rev. B* **1996**, *54* (16), 11169–11186. https://doi.org/10.1103/PhysRevB.54.11169.

(51) Kresse, G.; Joubert, D. From Ultrasoft Pseudopotentials to the Projector Augmented-Wave Method. *Phys. Rev. B* **1999**, *59* (3), 1758–1775. https://doi.org/10.1103/PhysRevB.59.1758.

(52) Blöchl, P. E. Projector Augmented-Wave Method. *Phys. Rev. B* **1994**, *50* (24), 17953–17979. https://doi.org/10.1103/PhysRevB.50.17953.

(53) Perdew, J. P.; Burke, K.; Ernzerhof, M. Generalized Gradient Approximation Made Simple. *Phys. Rev. Lett.* **1996**, *77* (18), 3865–3868. https://doi.org/10.1103/PhysRevLett.77.3865.

(54) Grimme, S.; Ehrlich, S.; Goerigk, L. Effect of the Damping Function in Dispersion Corrected Density Functional Theory. *J. Comput. Chem.* **2011**, *32* (7), 1456–1465. https://doi.org/10.1002/jcc.21759.

(55) Vorholz, J.; Harismiadis, V. I.; Rumpf, B.; Panagiotopoulos, A. Z.; Maurer, G. Vapor+liquid Equilibrium of Water, Carbon Dioxide, and the Binary System, Water+carbon Dioxide, from Molecular Simulation. *Fluid Phase Equilibria* **2000**, *170* (2), 203–234. https://doi.org/10.1016/S0378-3812(00)00315-0.

(56) Jain, A.; Ong, S. P.; Chen, W.; Medasani, B.; Qu, X.; Kocher, M.; Brafman, M.; Petretto, G.; Rignanese, G.-M.; Hautier, G.; Gunter, D.; Persson, K. A. FireWorks: A Dynamic Workflow System Designed for High-Throughput Applications. *Concurr. Comput. Pract. Exp.* **2015**, *27* (17), 5037–5059. https://doi.org/10.1002/cpe.3505.

(57) Momma, K.; Izumi, F. VESTA 3 for Three-Dimensional Visualization of Crystal, Volumetric and Morphology Data. *J. Appl. Crystallogr.* **2011**, *44* (6), 1272–1276. https://doi.org/10.1107/S0021889811038970.

(58) Forrest, K. A.; Pham, T.; Elsaidi, S. K.; Mohamed, M. H.; Thallapally, P. K.; Zaworotko, M. J.; Space, B. Investigating CO2 Sorption in SIFSIX-3-M (M = Fe, Co, Ni, Cu, Zn) through Computational Studies. *Cryst. Growth Des.* **2019**, *19* (7), 3732–3743. https://doi.org/10.1021/acs.cgd.9b00086.

(59) Ziaee, A.; Chovan, D.; Lusi, M.; Perry, J. J.; Zaworotko, M. J.; Tofail, S. A. M. Theoretical Optimization of Pore Size and Chemistry in SIFSIX-3-M Hybrid Ultramicroporous Materials. *Cryst. Growth Des.* **2016**, *16* (7), 3890–3897. https://doi.org/10.1021/acs.cgd.6b00453.

(60) Elsaidi, S. K.; Mohamed, M. H.; Simon, C. M.; Braun, E.; Pham, T.; Forrest, K. A.; Xu, W.; Banerjee, D.; Space, B.; Zaworotko, M. J.; Thallapally, P. K. Effect of Ring Rotation upon Gas Adsorption in SIFSIX-3-M (M = Fe, Ni) Pillared Square Grid Networks. *Chem. Sci.* **2017**, *8* (3), 2373–2380. https://doi.org/10.1039/C6SC05012C.

(61) Zhao, P.; Lampronti, G. I.; Lloyd, G. O.; Suard, E.; Redfern, S. A. T. Direct Visualisation of Carbon Dioxide Adsorption in Gate-Opening Zeolitic Imidazolate Framework ZIF-7. *J. Mater. Chem. A* **2014**, *2* (3), 620–623. https://doi.org/10.1039/C3TA13981F.

(62) Elsaidi, S. K.; Mohamed, M. H.; Schaef, H. T.; Kumar, A.; Lusi, M.; Pham, T.; Forrest, K. A.; Space, B.; Xu, W.; Halder, G. J.; Liu, J.; Zaworotko, M. J.; Thallapally, P. K. Hydrophobic Pillared Square Grids for Selective Removal of CO2 from Simulated Flue Gas. *Chem. Commun.* **2015**, *51* (85), 15530–15533. https://doi.org/10.1039/C5CC06577A.

(63) Zhu, A.-X.; Lin, J.-B.; Zhang, J.-P.; Chen, X.-M. Isomeric Zinc(II) Triazolate Frameworks with 3-Connected Networks: Syntheses, Structures, and Sorption Properties. *Inorg. Chem.* **2009**, *48* (8), 3882–3889. https://doi.org/10.1021/ic802446m.

(64) Deria, P.; Li, S.; Zhang, H.; Snurr, R. Q.; Hupp, J. T.; Farha, O. K. A MOF Platform for Incorporation of Complementary Organic Motifs for CO2 Binding. *Chem. Commun.* **2015**, *51* (62), 12478–12481. https://doi.org/10.1039/C5CC04808G.

(65) Shimomura, S.; Matsuda, R.; Kitagawa, S. Flexibility of Porous Coordination Polymers Strongly Linked to Selective Sorption Mechanism. *Chem. Mater.* **2010**, *22* (14), 4129–4131. https://doi.org/10.1021/cm101410h.

(66) Shimomura, S.; Higuchi, M.; Matsuda, R.; Yoneda, K.; Hijikata, Y.; Kubota, Y.; Mita, Y.; Kim, J.; Takata, M.; Kitagawa, S. Selective Sorption of Oxygen and Nitric Oxide by an Electron-Donating Flexible Porous Coordination Polymer. *Nat. Chem.* **2010**, *2* (8), 633–637. https://doi.org/10.1038/nchem.684.

(67) Tan, Y.-X.; He, Y.-P.; Wang, M.; Zhang, J. A Water-Stable Zeolite-like Metal–Organic Framework for Selective Separation of Organic Dyes. *RSC Adv.* **2013**, *4* (3), 1480–1483. https://doi.org/10.1039/C3RA41627E.

(68) Quiñonero, D.; Frontera, A.; Deyà, P. M. Feasibility of Single-Walled Carbon Nanotubes as Materials for CO2 Adsorption: A DFT Study. *J. Phys. Chem. C* **2012**, *116* (39), 21083–21092. https://doi.org/10.1021/jp306586f.

(69) Lísal, M.; Smith, W. R.; Nezbeda, I. Accurate Vapour–Liquid Equilibrium Calculations for Complex Systems Using the Reaction Gibbs Ensemble Monte Carlo Simulation Method. *Fluid Phase Equilibria* **2001**, *181* (1), 127–146. https://doi.org/10.1016/S0378-3812(01)00489-7.

(70) Pettinari, C.; Tăbăcaru, A.; Boldog, I.; Domasevitch, K. V.; Galli, S.; Masciocchi, N. Novel Coordination Frameworks Incorporating the 4,4′-Bipyrazolyl Ditopic Ligand. *Inorg. Chem.* **2012**, *51* (9), 5235–5245. https://doi.org/10.1021/ic3001416.

TOC Graphic

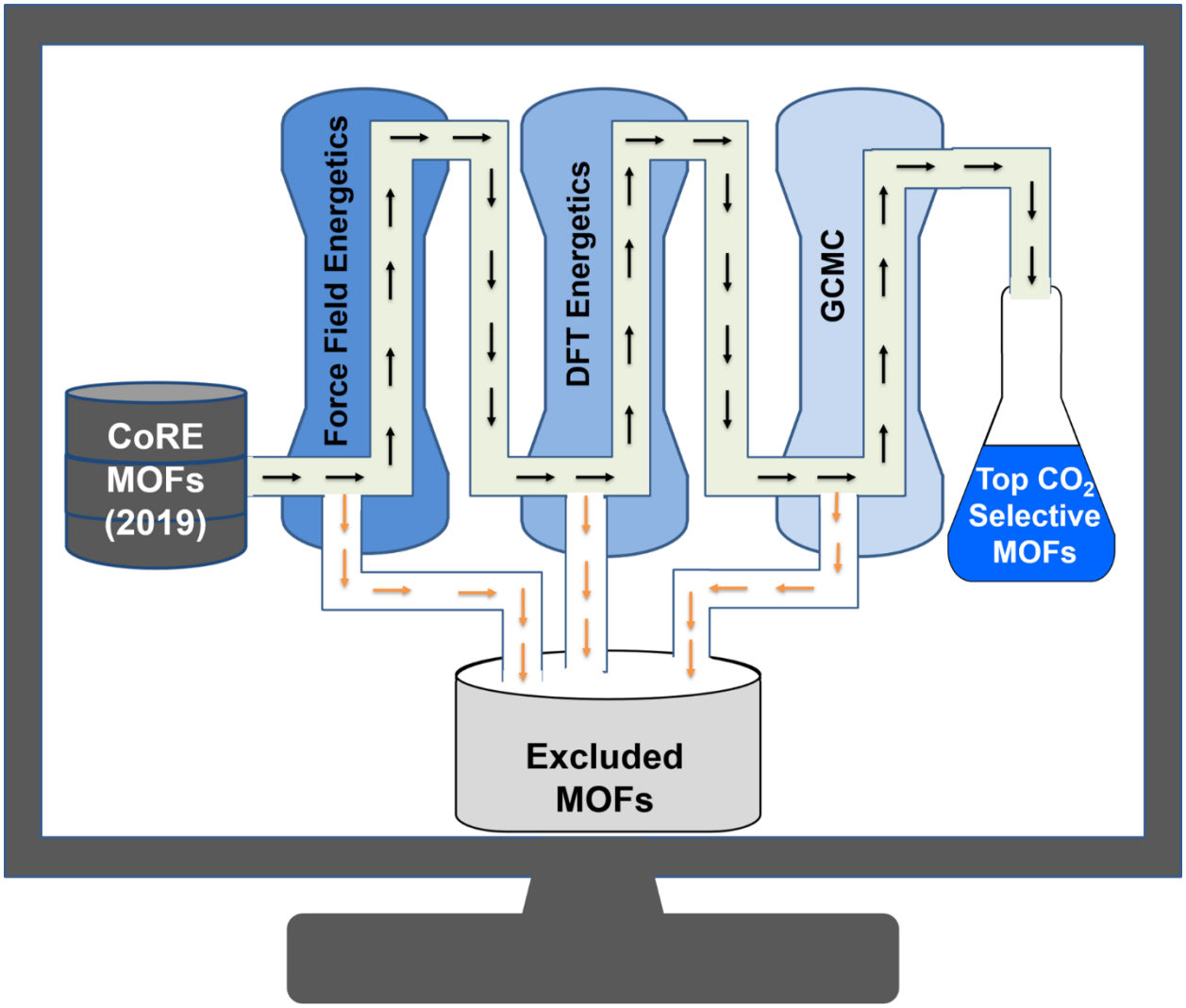
CoRE
MOFs
(2019)
Force Field Energetics
DFT Energetics
GCMC
Top CO_2
Selective
MOFs
Excluded
MOFs